DESIGN OF AN EXPERIMENTAL ABLATIVE PULSED PLASMA THRUSTER FOR MICROPROPULSION

17 – 18 – 19 MARCH 2021

S. Barquero[1], **M. Merino**[2], **J. Navarro Cavallé**[1]
[1]Equipo de Propulsión Espacial y Plasmas, Universidad Carlos III de Madrid, Leganés, Spain,
mbalsera@ing.uc3m.es

KEYWORDS: Ablative Pulsed plasma thrusters, micropropulsion

ABSTRACT:

A versatile ablative pulsed plasma thruster (APPT) experiment is presented, intended to study the low-power operation of this technology for micropropulsion missions. The design requirements, constraints and objectives are discussed, detailing in particular the parametric range that will be investigated in an upcoming test campaign. The main driver in all design choices is the flexibility and agility to enable the fast modification of the experiment. The subsystems required by the thruster operation are examined, and a simple model is used to estimate the expected propulsive performance. Finally, the planned next steps in this study are reviewed.

1. INTRODUCTION

A new low-power APPT is being developed for CubeSat micropropulsion in the frame of the regional MARTINLARA project. The advantages of using an ablative pulsed plasma thruster derive from its simple technology, with less complexities to be scaled down in comparison with other electric thrusters. CubeSat limitations lie in supplied power and size. The firing frequency is mainly constrained by the available power and the power capability of the electronic components involved. We target to integrate our thruster in 1U.

Since the first Soviet Zond probes - were launched at the mid 60s –coaxial/50J/1kV (also the igniter)– , different research groups have been working on APPT developments. The improvement of its technology together with the growing exploitation of increasing small spacecrafts created chances for APPT to play primary propulsive roles; in addition, the attention was focused on the under-20J operation energy range. Historically, highlighted research lines qualified to fly correspond to the LES 6 –1-10J– and 8/9 –80J/1.5-3kV– missions developed by the MIT [1–4], as well as the throttleable APPT of the SMS mission [5, 6] or the TIP II from NOVA series [6, 7] –20J– missions; all of them were a prelude of the improved E0-1 [6, 8, 9]. Since the 90s, the RIAME resumed the old Soviet studies; their thrusters range between 20-155J [10, 11]. Efforts done by The Princeton University during 90s and 2000s over gas-fed channels helped also to understand the pulsed discharge phenomena [12–15]. The investigations done around SIMP-LEX [16–23], developed principally by the IRS, have been decisive for recent μAPPT promising proposals, as its own one, the coaxial Petrus device [24, 25]. Another one of the latest series of fruitful experiments, but parallel rail, has been starred by the PPTCUP CubeSat thruster module and the derivatives of the research line associated, carried out between La Sapienza and the Southaptom University [26–30] – finally with commercial applications. Most published APPTs are parallel rail; Tab. 1 collects a representative sample of low scale parallel rail μAPPTs under 10 J used as reference for the current design –different breadboard models and/or derivatives associated to each respective research line were also developed.

Thruster	W_0 [J]	W_0/A [J/cm^2]	V [V]	c [μF]	Isp [s]	Ibit [μNs]
LES-6 (B) [1–4, 6]	<7 (1.85)	<2.6	500-2000	0.66 -6	590 (300)	<90 (26)
SMS (B) [6]	8.4	1.15	-	-	450	133
EO-1 (B) [6, 31]	<10 (8.5)	0.88	-	-	650	<100 (90)
Dawgstar (B) [31, 32]	5.23	2.27	500-2000	-	483	56
PPT-B20/TMIT-X (B) [33, 34]	2.3-3.6 (3.38)	(6.76)	1500	1-3	(960)	(22)
STSAT-2 (B) [35]	1.8	-	>1500	1.6	800	25
PPTCUP (S) [26–30]	(1.7)	(2-2.3)	<1500	2.4-3.2/ SP: 333pF	590	(29)
BIT* (B) s [36–38]	-	-	<1500	(2)/ SP: 0.18μF	-	-

Table 1: Parallel rail μAPPT used as reference. Values between brackets correspond to nominal operation points published and ranges/no-brackets values are based on experimental study data. (*) It also studies double discharge. Legend: (B)-Breech-fed, (S)-Side-fed/ SP-Spark plug. The channel size varies from a device to another one, but is generally based on the magnitude order of the cm; often, the height is larger than the width and cathode and anode share the same length. Usually, the channels are covered, involving also a nozzle. Common magnitude order for initial resistance in mΩ and initial inductance in nH. Firing frequency based on 1 Hz. Thrust efficiency under 10%.

The main goal of the present design is to serve as a versatile experimental platform to test low-power

APPT technology. In order to gain understanding of the APPT discharge and optimize the final thruster design, an intermediate step is to design, build and test a adaptable low-power APPT experiment that enables us to explore different geometries, design parameters, and operating ranges.
In Section 2., the main design requirements, constraints and objectives used to define the design point are mentioned. Section 3. introduces the mechanical and electrical architecture, and a simple model is used to estimate the expected propulsive performance –in addition, considerations about more accurate modeling are included. Finally, Section 4. presents the planned next steps in this experimental study.

2. DESIGN POINT

The developed device is a parallel-rail APPT that allows the modification of: the geometric characteristics of the thruster head, the configuration of the power electronics, and the operation point. Tab. 2 summarizes the intended ranges of variation of the design and operational parameters. These values were selected based on approximate scaling laws derived by inspection of existing APPTs for microsatellites of the same class. Critical starting considerations deal with geometry and size, input power and available energy over propellant exposed area ratio (W_0/A), together with breakdown voltage and triggering method and associated parameters –both, particularized for the geometrical configuration and materials of interest.

Nomenc.	PARAMETER	Unit	Nominal point	Modification range
h	Channel height	[cm]	1	<2
A_w	Propellant section width	[cm]	1	<2
l	Channel length	[cm]	3	1-5
V	Electrode voltage	[kV]	1	0.5-2.5
V_{SP}	Spark plug voltage	[kV]	2	<6
W_0/A	Available Energy/propellant surface ratio	[J/cm2]	2	<4
W_0	Available Energy	[J]	2	<10
C	Capacitance	[μF]	4	<10
V_{in}	Voltage input*	[V]	-	<20
P_{in}	Input power*	[W]	-	<20
f_{firing}	Firing frequency	[Hz]	1	-

Table 2: Design central point.Tapering and flaring angles allowed for main electrodes. Spark plug/anode height and spark plug/propellant surface distance modifiable. (*) Satellite bus common operational values.

Discharge channel entails rectangular –flaring and tapering angles allowed– electrodes elongated axially. It has been seen that the W_0/A ratio can differ noticeably with each prototype, they do not scale proportional with energy; as well as, the resultant performance results for comparable scenarios also does, which could engage high influence of geometrical aspects on the performance. For the main electrode voltage drop, we take the range 500-2000V (1kV nominal) as a conservative testing margin. The basis for sizing regarding the energy and the capacitance are set as a compromise solution bounded by the demands over the mechanical and electrical architecture that a device within the context of micropropulsion can bear. Hence, considering the mentioned necessary voltage drop, numerous low-power APPTs for CubeSat operation are placed under 10J and, subsequently, µF capacitances; it places the discharges into the underdamped regime, a less demanding scenario –see Section 3.3.W_0/A does not scales strictly with stored energy; typical values for this energy range and parallel-rail APPTs are commonly placed under 4 J/cm^2. The trigger voltage ranges widely, specially for testing purposes, but can be nominally based around 1kV for devices which contain spark plugs with sharp geometries. Even though, endurance tests have been also performed at higher potential,to be one step ahead of the difficulties to ignite associated to degradation, in order to gain lifetime reliability [39]. Maximum input power around 20W is coherent with usual CubeSat power capability.

Apart from the previous constraints, additional needs and requirements apply. Derived from the study purpose, the prototype shall be operated in modifiable Impulse bit from 10-100 µNs, hence, electrical and geometrical parameters shall be modifiable to determine their influence on the discharge, in addition to materials. Regarding electrical parameters: capacitance, electrode voltage and available energy for the spark plug and main electrodes; in case of geometrical ones: propellant section in terms of width and height and inclination angle of its surface, channel width, height, length, flaring angle and tapering angle as well as the spark plug configuration and position, and the discharge circuit initial inductance and resistance, relative position (and/or shape) of the insulating elements. As well, important requirements are easiness to iterate (fast acceptance of modifications, geometry variations and repetitive assembly and disassembly without degradation) and easiness of manufacturing. The first breadboard prototype we consider for this studywill be tested inside a vacuum chamber of 50x50x50cm –considering, in turn, the access to its inside is limited by a 25cm-diameter window–, so, the high level requirement in size, 1U, does not apply at the current development phase.

Appropriate materials must be vacuum suitable, possess very low outgassing rate, be structurally strong enough to thermal loads be manufacture-friendly and match with the specific functionality of such piece. Regarding the latest, main demands fall on: conductivity and structural aspects for the main electrodes, emissivity for the spark plug, insulation capability and thermal resistance for the insulating pieces and a useful point for sublimation in the case of a non-aggressive propellant.

3. DESIGN ARCHITECTURE

In order to gain independence between the different subsystems and facilitate iteration, a modular solution is presented. The experimental proposal involves the following subsystems: 1) the thruster head, 2) the power electronics, 3) control and sensing, and 4) the structure. A summary of the subsystems along next subsections. Fig. 1 shows CAD and real views of the developed APPT breadboard.

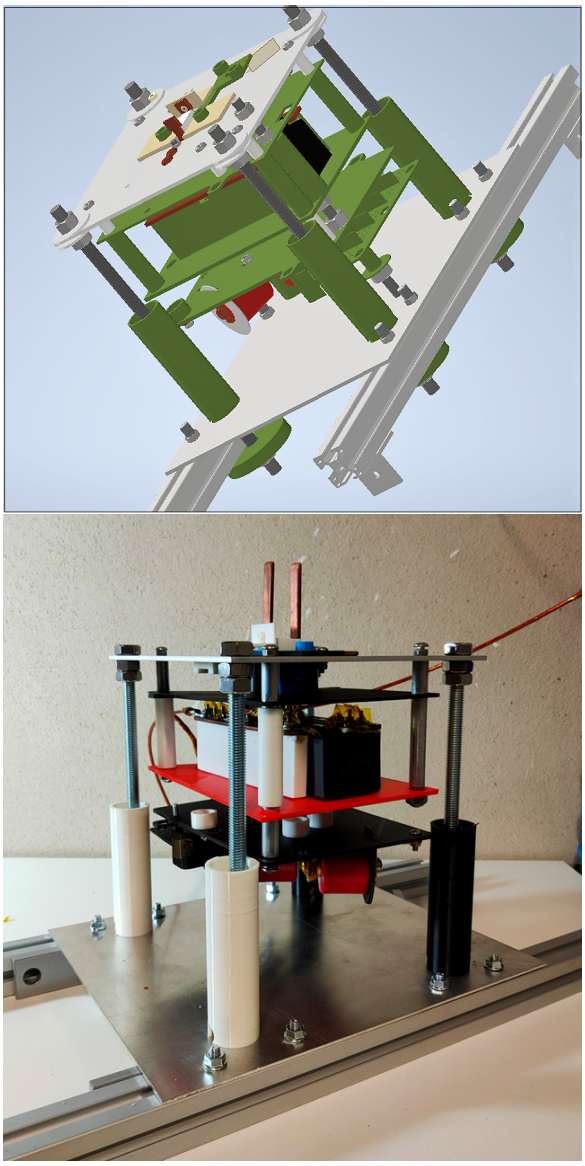

Figure 1: APPT breadboard system: CAD and Real view. The system includes the experimental platform with all its subsystems and the structural setup to hold it -suitable to be placed inside the vacuum chamber. In the CAD view, grey and brown colors correspond to conductive materials.

Made of aluminium, the structure provides a robust envelope for the thruster head and electronic boards. A design based on modular levels that, in turn, keeps the thruster skeleton at sight, facilitates the manipulation and modification of different elements independently. Mechanical and electrical interfaces compatible with the vacuum chamber are provided. For mitigating electrical hazards, the anode (thruster head) is grounded to the chassis of the structure, which in turn is connected to the vacuum chamber ground.

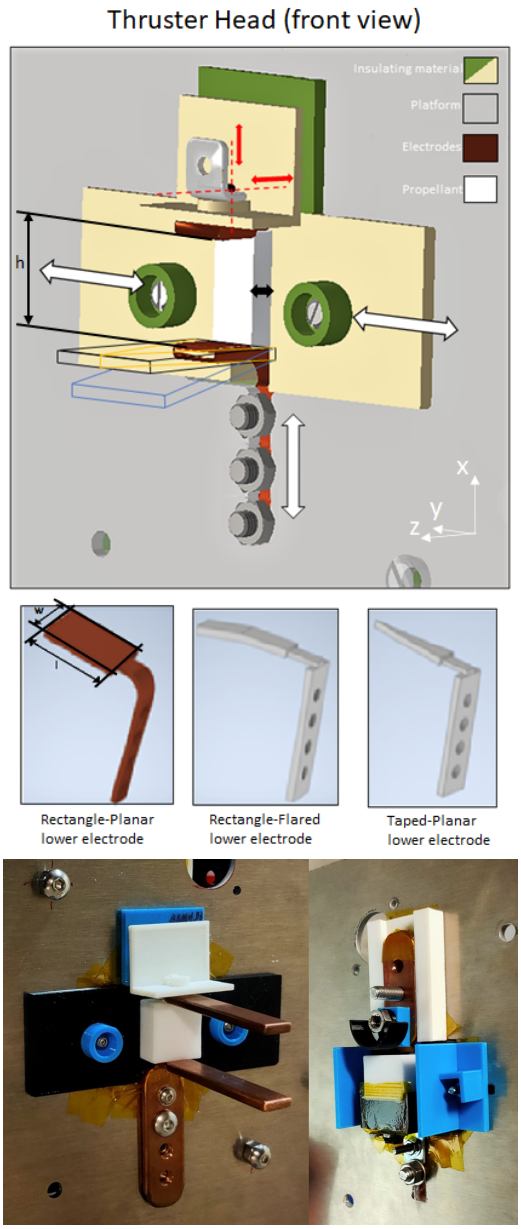

Figure 2: Thruster head. CAD representation includes information about the geometry modifications allowed. Legend: length (l), height (h) and width (w). Degrees of freedom on the assembly of electrodes and propellant, are represented by arrows. The shape of the upper electrode can be modeled as the lower one, just considering the spark plug hosting. The flaring and taping geometries offer extra degrees of freedom in the design, angles and length. This representation corresponds to the uncovered channel version.

3.1. THRUSTER HEAD

The thruster head –see Fig. 2– is based on two electrodes (cathode and anode) which extend axially defining a parallel rail channel, fed from its

breech. Besides, the cathode accounts with the incorporation of an insulated spark plug, whose anode role is played by the lower electrode too.
To make the design versatile the current design allows geometrical variation to cover the ranges shown in Tab. 2. Acceptation of modifiable propellant section (in terms of height and width) is enabled through the displacement of the structural insulating casing pieces. The channel geometry can be,in turn, modified through the exchange of the electrodes, whatever their shape is, while their connection section shape is respected. Interesting studies deal with the variation of the propellant surface (area, properties, inclination angle...), W_0/A ratio, channel height/width/length, flaring/tapering electrode angles and spark plug configuration and relative position. The design is compatible with both, naked and covered discharge channel through the modification of the shape of the insulating pieces.
Different materials will be studied for the electrodes and the insulating elements in direct contact with the plasma.

3.2. POWER ELECTRONICS

The power segment of the PPU is based on a pulse forming network that makes use of two analogous circuits, one associated to the main electrodes and the spark plug circuit. The degree of independence of the experimental spark plug and main circuits in terms of power electronics can be discussed. Two stages are distinguished to deal respectively with the charge and the discharge processes (entailing the plasma side).
Battery charging is fundamental to enable a potential scenario for further development of a short-time low-power discharge. A voltage elevation preconditioner is needed when a low-voltage power supply is used (as a representative of the satellite bus). EMCO DC-DC isolated converters have been considered for this purpose -FS30 and E60 models. The discharge circuit connects, respectively, each battery with the corresponding electrodes. To improve efficiency, initial resistance of the main circuit shall be smaller than the inductance slope and the minimization of its initial inductance shall share magnitude order with the total inductance increment. Using diodes, current reversal is prevented to happen along the spark plug circuit in case of underdamped plasma discharge (even though this current is expected to be very low).
Capacitance, electrode voltage and pulse energy modifications are allowed in both circuits. The maximum pulse repetition frequency is limited by the main battery charge time, depending on the input power at the DC-DC module and its capabilities, in case of being used.
It has to exist a coordination between spark plug operation and the charge level of the main battery. Different control schemes apply to provide controllable firing.

3.3. PERFORMANCE ESTIMATE

To find the matching point between the dynamic impedance of the discharge and the output impedance of the source, electrical models to approximate the plasma behavior are widely used as starting reference frame for design. The models are derived from simplified versions of the plasma momentum conservation equation and the series RLC circuit equation [40]:

$$\frac{\mathrm{d}}{\mathrm{d}t}\left(m\frac{\mathrm{d}z}{\mathrm{d}t}\right) = \iiint \mathbf{J}\times\mathbf{B}\ \mathrm{d}V\Big]_z = \frac{1}{2}\frac{\mathrm{d}L}{\mathrm{d}z}\ J^2 \quad \text{Eq. 1}$$

$$0 = \frac{1}{C}\ J_x + \frac{\mathrm{d}}{\mathrm{d}t}\left(L\frac{\mathrm{d}J}{\mathrm{d}t} + J\frac{\mathrm{d}L}{\mathrm{d}t}\right) + \frac{\mathrm{d}}{\mathrm{d}t}(R\ J) \quad \text{Eq. 2}$$

where z and x refer to the axial and cross directions respectively. t dependence has not been specified in order to simplify. $L_p(t) = (\mu_0\frac{h}{w})z(t)$ for parallel plates with $h/w << 1$.
The momentum equation (1) assumes the locally-concentrated nature of the plasma density distribution as a sheet of negligible thickness with constant properties within its entire volume -properties at the channel center line- being completely axially current free, (2) the sheet is completely ionized due to the high enough current density (fro the beginning, as the ionization stage time scale is assumed negligible) and just one population of ions is taken into account, (3) takes the 1D approximation at the channel center, deprecating edge effects and derivatives along the cross directions,(4) as width is much larger than height, magnetic field lines can be assumed perpendicular to the current, and so, Lorentz force always point towards the channel exit, and (5) in general, as the model lays aside specific terms for particle interaction or pressure terms (cold ions), it does not allowing for any recovery of thermal energy. The Snowplow model keeps the time-dependent mass term in Eq. 1 to represent the dynamical losses due to the entrainment of neutrals (as neutrals are skipped in this formulation) as the sheet advances downstream through a channel expected to be filled by the ablation/desorption of the propellant external layers. Regarding the RLC circuit equation, the plasma sheet is considered as a resistance –commonly constant, as total ionization is assumed since the beginning– and a time-dependent inductance term. This resistance displaces along the channel by the dynamics described in the momentum equation.
Fig. 3 shows the solution of the Snowplow model applied to the nominal point 1000V/4μF battery (2J), with an initial circuit inductance (L_0) of 10nH, assuming the plasma sheet resistance constant with

a total value for the whole circuit (R) of 10mΩ and involving an initial mass bit of 1ug. In Fig. 4, a parameterization respect to the nominal case concerning capacitance, initial resistance and initial inductance variations is presented. Initial inductance and resistance magnitude orders come from the electrical efficiency definition, favoring its maximization –proportion of stored energy that has been converted completely into kinetic energy to the plasma layers, assuming the resistive term as losses. Using the LC solution as boundary, this efficiency can be expressed as a ratio between inductances ($\eta_e < \Delta L/L_0$), useful for sizing. The optimal energy transfer happens at the critical damping value of capacitance, however, low-power APPTs usually operate underdamped as the critical capacitance is several orders of magnitude over the µF regime (common for this class) and the current peak and rise time are lower and, so, more suitable for miniaturized thrusters. Empirical evidence about the attachment of these softer secondary discharges under most of conditions, corroborates that the efficiency tends to drop after the first peak, as the electrical energy transfer into kinetic one rate also does. However, the avoidance of the overdamped solution resides on the reduction on the demands over the thruster architecture. The smaller is the ratio $(C^2V^2(\mathrm{d}L/\mathrm{d}z)^2)/_0L_0$, the smaller will be also the damping ratio, which, in turn, increases with the resistance. With this data, a fast estimation of the instantaneous impulse ($I_{bit} \approx 1/2 \mathrm{d}L/\mathrm{d}z J^2_{peak}\ \mathrm{d}t$) and the specific impulse ($I_{sp} \approx u_{peak}/g_0$) can be done; results included in Tab. 3 for the cases depicted in Fig. 3.

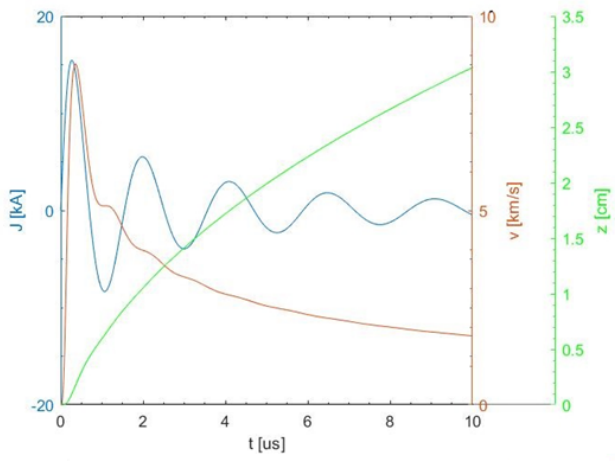

Figure 3: Nominal point estimated performance. Values: 1000V/4uF (2J), h/w=1 (and 10m ■, 10nH, 1ug. Channel density considered to compute the mass entrained by the sheet as it advances set in 0.0165 kg/m^3, as an approximation for TEFLON. The computation does not consider edge effects due to the finite electrode width.
h/w =1. The error of the inductance slope expression taken minimizes with h<<w.

		Nominal case	Inductance increment	Resistance increment	Capacitance increment
Current peak	[kA]	15.5	6	7	20
Ibit	[µNs]	38	6	8	62
Isp	[s]	895	345	380	1192

Table 3: Current peak, impulse bit and specific impulse for the cases represented in Fig. 3. dt= 0.25 us for the computation of I_{bit}.

Efforts to describe the physics of PPTs have been so far limited, and there is a sore lack of models that include plasma physics; existing models are mainly electric [1,6,12,26,40–42]. Potential benefits would be extracted from improvements on plasma models with the aim of getting self-consistent codes. In parallel to this experimental activity, a numerical multifluid transient model –suitable approach at the high electron density limit, 10^{19}-10^{20} for close-to-5J operation [43]– is being developed,in order to provide the time evolution of the plasma parameters (such as density, electron potential, electron temperature, ions and neutrals velocity, and electric current and magnetic field) along the acceleration channel volume. This code would allow our team to perform parametric studies of the APPT design/operational parameters, and their impact on the thruster performances. The on-going numerical work is being addressed based on the Method of the Characteristics (including the treatment of fluid discontinuities), and multiple programming architectures and numerical schemes have been tried.

4. NEXT STEPS

The present design is part of an open experimental study. Ultimate goals focus on the better understanding of the physics of the low-power APPT discharge and to provide experimental data in order to validate numerical models being developed in parallel to this activity –Section 3.3.. Last but not least, this versatile platform should simplify the experimental optimization of a low-power class APPT. The thrust to power ratio optimization is expected to be associated to the optimization of the momentum electromagnetic component much more than taking advantage of the pressure gradient contribution. Other optimization tasks of interest are the improvements on design simplicity and robustness, reduction of size and weight, long lifetime (more uniform ablation, slighter degradation of the electrodes and PPU, shielding against firing contamination, gaining spark plug reliability...) or ensuring repeatabiliy, controllability and predictability of the impulse bit.
The focus of the first experimental campaign is to characterize the macroscopic behavior of the discharge. It will emphasize on (1) the electrical characterization of the discharge –monitoring the temperature, voltage and direct current measurements–, (2) the plasma characterization in z,x,t (mainly

species densities, velocities and induced B field) together with (3) the visual inspection of the thruster components after firing. Planned tests over the generated fluid are, in principle, time-resolved Langmuir probes, using triple or quadruple arrangements, time-of-flight measurements (using single Langmuir probes). B-dot probes and optical diagnostics as emission spectroscopy and fast camera. Finally, also direct measurements of the thrust will be accomplished through an impulsive balance being developed on-purpose.
The data gathered in this experimental campaign will help improving the low-power APPT experiment, and ultimately, will be used to design an electrically throttleable APPT unit suitable for Cubesats.

5. ACKNOWLEDGMENTS

This work was been supported by the MARTINLARA project, funded by the Comunidad de Madrid, under Grant reference P2018/NMT-4333 MARTINLARA-CM.

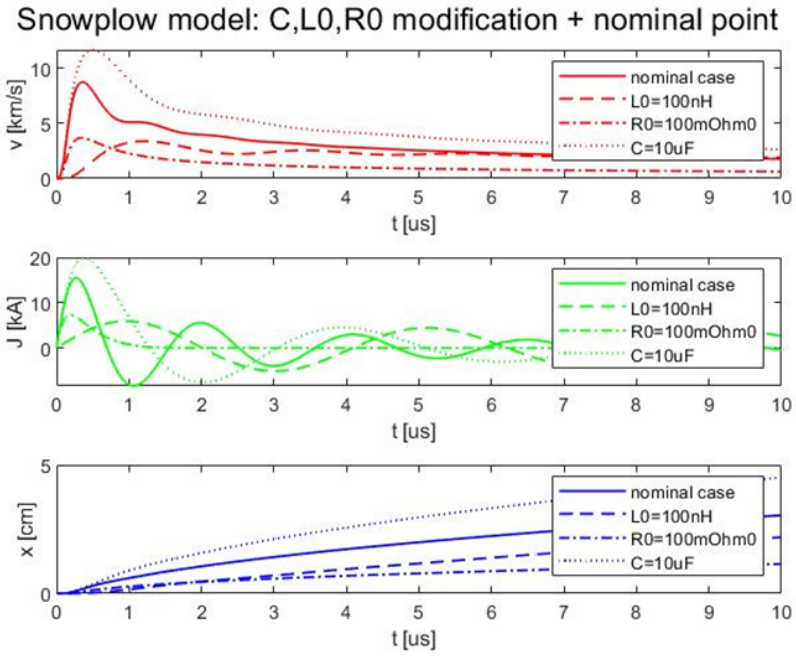

Figure 4: Snowplow model dimensional solution based on the design point. Nominal point: 1000V/4μF (2J),1x1cm channel section and 10mΩ,10nH,1ug. Channel density considered to compute the mass entrained by the sheet as it advances set in 0.0165 kg/m^3, as an approximation for TEFLON.
The computation does not consider edge effects due to the finite electrode width.
h/w =1. The error of the inductance slope expression taken minimizes with h<<w.

6. REFERENCES

[1] SOLBES, A., Thomassen, K., and VONDRA, R. J., "Analysis of solid teflon pulsed plasma thruster," *Journal of Spacecraft and Rockets*, Vol. 7, No. 12, 1970, pp. 1402–1406.

[2] Vondra, R., Thomassen, K., and Solbes, A., "A pulsed electric thruster for satellite control," *Proceedings of the IEEE*, Vol. 59, No. 2, 1971, pp. 271–277.

[3] Guman, W. J. and Nathanson, D. M., "Pulsed Plasma Microthruster Propulsion System for Synchronous Orbit Satellite," *J. Spacecraft*, Vol. 7, No. 4, 1970, pp. 409–415.

[4] Guman, W. J., "Solid Propellant Pulsed Plasma Propulsion System Design," *J. Spacecraft*, Vol. 13, No. 1, 1976, pp. 51–53.

[5] Guman, W. J. and Williams, T. E., "Pulsed plasma microthruster for synchronous meteorological satellite," *Journal of Spacecraft and Rockets*, Vol. 11, No. 10, 1974, pp. 729–731.

[6] Burton, R. and Turchi, P., "Pulsed plasma thruster," *J. Propulsion and Power*, Vol. 14, 1998, pp. 716–735.

[7] EBERT, W., KOWAL, S., and SLOAN, R., "Operational Nova spacecraft teflon pulsed plasma thruster system," *25th Joint Propulsion Conference*, 1989, p. 2497.

[8] Arrington, L. A., Haag, T. W., Pencil, E. J., and Meckel, N. J., *A performance comparison of pulsed plasma thruster electrode configurations*, National Aeronautics and Space Administration, Lewis Research Center, 1997.

[9] Zalawski, C., Benson, S., Smernan, P., and Hoskins, A., "On-Orbit Testing of the EO-1 Pulsed Plasma Thruster," .

[10] Antropov, N., Bogatyy, A., Dyakonov, G., Lyubinskaya, N., Popov, G., Semenikhin, S., Tyutin, V., Khrustalev, M., and Yakovlev, V., "A new stage in the development of ablative pulsed plasma thrusters at the RIAME," *Solar System Research*, Vol. 46, No. 7, 2012, pp. 531–541.

[11] Antropov, N., Bogatyy, A., Boykachev, V., Dyakonov, G., Lyubinskaya, N., Popov, G., Semenikhin, S., Tyutin, V., and Yakovlev, V., "Development of Russian Next-generation Ablative Pulsed Plasma Thrusters," *Procedia engineering*, Vol. 185, 2017, pp. 53–60.

[12] Ziemer, J. and Choueiri, E., "Dimensionless performance model for gas-fed pulsed plasma thrusters," *34th AIAA/ASME/SAE/ASEE Joint Propulsion Conference and Exhibit*, 1998, p. 3661.

[13] Ziemer, J., Choueiri, E., and Birx, D., "Comparing the performance of co-axial and parallel-plate gas-fed PPTs," *26th International Electric Propulsion Conference, Kitakyushu, JAPAN*, 1999, pp. 99–209.

[14] Berkery, J. and Choueiri, E. Y., "Canted current sheet mass leakage and its impact on pulsed plasma thruster performance," *40th AIAA Joint Propulsion Conf., Fort Lauderdale, FL*, 2004.

[15] Markusic, T. E., Berkery, J. W., and Choueiri, E. Y., "Visualization of current sheet evolution in a pulsed plasma accelerator," *IEEE Transactions on Plasma Science*, Vol. 33, No. 2, 2005, pp. 528–529.

[16] Nawaz, A., Lau, M., G, H., and Auweter-Kurtz, M., "Investigation of the Magnetic Field in a Pulsed Plasma Thruster," *AIAA Journal*, Vol. 46, No. 11, 2008, pp. 2881–2889.

[17] Nawaz, A., R, A., and Auweter-Kurtz, M., "Thrust efficiency optimization of the pulsed plasma thruster SIMP-LEX," *Acta Astronautica*, Vol. 46, No. 11, 2008, pp. 2881–2889.

[18] Schönherr, T., Komurasaki, K., Kawashima, R., Arakawa, Y., and Herdrich, G., "Evaluation of discharge behavior of the pulsed plasma thruster SIMP-LEX," *46th AIAA/ASME/SAE/ASEE Joint Propulsion Conference & Exhibit*, 2010, p. 6530.

[19] Schönherr, T., Nees, F., Koizumi, H., Arakawa, Y., Manna, S., Lau, M., Herdrich, G., and Fasoulas, S., "Mass and Plasma Characteristics in the Current Sheet of a Pulsed Plasma Thruster," 09 2011.

[20] Sch́onherr, T., Nees, F., Arakawa, Y., Komurasaki, K., and Herdrich, G., "Characteristics of plasma properties in an ablative pulsed plasma thruster," *Physics of Plasma*, Vol. 20, No. 3, 2013, pp. 033503.

[21] Lau, M., Manna, S., Herdrich, G., Schönherr, T., and Komurasaki, K., "Investigation of the plasma current density of a pulsed plasma thruster," *Journal of Propulsion and Power*, Vol. 30, No. 6, 2014, pp. 1459–1470.

[22] Schönherr, T., Stein, M., Komurasaki, K., and Herdrich, G., "Observation of discharge arc properties in pulsed plasma thruster," *2014 International Symposium on Discharges and Electrical Insulation in Vacuum (ISDEIV)*, IEEE, pp. 705–708.

[23] Schönherr, T., Stein, M., Komurasaki, K., and Herdrich, G., "Investigation of discharge arc phenomena in ablative PPT," *IEPC-2015-79*, 2015.

[24] Montag, C., Burghaus, H., Herdrich, G., and Schönherr, T., "Development of a new Pulsed Plasma Thruster and a Brief Introduction of a Planned Test Facility," *67th Int. Astronaut. Congr*, 2016, pp. 1–15.

[25] Montag, C., Herdrich, G., and Schönherr, T., "Modifications and experimental analysis towards an update of the pulsed plasma thruster PETRUS," *Proceedings of the 35th International Electric Propulsion Conference, Atlanta, GA, USA*, 2017, pp. 8–12.

[26] Guarducci, F., Coletti, M., and Gabriel, S., "Design and testing of a micro pulsed plasma thruster for Cubesat application," *32nd International Electric Propulsion Conference*, 2011, pp. 2011–239.

[27] Coletti, M., Guarducci, F., and Gabriel, S. B., "A microPPTforCubesatapplication:Designandpreliminary experimentalresults," *Acta Astronautica*, Vol. 69, 2011, pp. 200–208.

[28] Ciaralli, S., Coletti, M., Guarducci, F., and Gabriel, S., "PPTCUP lifetime test results," *33rd International Electric Propulsion Conference, Washington DC, USA*, Citeseer, 2013.

[29] Mingo Perez, A., Coletti, M., and Gabriel, S., "A micro PPT for Nano-satellite applications: Design and experimental results," *48th AIAA/ASME/SAE/ASEE Joint Propulsion Conference & Exhibit*, 2012, p. 4279.

[30] Coletti, M., Ciaralli, S., and Gabriel, S. B., "PPT development for nanosatellite applications: Experimental results," *IEEE Transactions on Plasma Science*, Vol. 43, No. 1, 2014, pp. 218–225.

[31] Cassady, R., Hoskins, W., Campbell, M., and Rayburn, C., "A micro pulsed plasma thruster (PPT) for the 'Dawgstar' spacecraft," *Aerospace Conference Proceedings*, Vol. 4, IEEE, Piscataway, NJ, 2000, pp. 7–14.

[32] Rayburn, C., Campbell, M., Hoskins, W., and Cassady, R., "Development of a micro pulsed plasma thruster for the Dawgstar nanosatellite," *36th AIAA/ASME/SAE/ASEE Joint Propulsion Conference and Exhibit*, 2000, p. 3256.

[33] Uezu, J., Iio, J., Kamishima, Y., Takegahara, H., Wakizono, T., and Sugiki, M., "Study on pulsed plasma thruster configuration to expand impulse bit range," *29th International electric propulsion conference*, Vol. 234, 2005.

[34] KUMAGAI, N., SATO, K., TAMURA, K., KAWAHARA, K., KOIDE, T., TAKEGAHARA, H., SUGIKI, M., WAKIZONO, T., and

HASHIMOTO, H., “RESEARCH AND DEVELOPMENT STATUS OF LOW POWER PULSED,” .

[35] Shinohara, S. and Tanikawa, T., “Characteristics of a large volume, helicon plasma source,” *Physics of Plasmas*, Vol. 12, 2005, pp. 044502.

[36] Huang, T., Wu, Z., Liu, X., Xie, K., Wang, N., and Cheng, Y., “Study of breakdown in an ablative pulsed plasma thruster,” *Physics of Plasmas*, Vol. 22, No. 10, 2015, pp. 103511.

[37] Wu, Z., Sun, G., Liu, Z., Liu, X., Xie, K., and Wang, N., “Characteristics of plasma properties in double discharge ablative pulsed plasma thrusters,” *Physics of Plasmas*, Vol. 24, No. 11, 2017, pp. 113521.

[38] Shangmin, W., Licheng, T., Weiwei, F., Tianping, Z., Xinwei, C., Changwen, C., Xingda, L., Jun, G., and Weidong, L., “μ-PPT electropropulsion system Development and First fight Application,” *system*, Vol. 1, 2017, pp. 9.

[39] GUARDUCCI, F., “Design and Testing of a Micro PPT for CubeSat Applications,” 2012.

[40] Jahn, R., *Physics of Electric Propulsion*, Dover, 2006.

[41] Ziemba, T., Winglee, R., and Euripides, P., “Parameterization of the Laboratory Performance of the Mini-Magnetospheric Plasma Propulsion (M2P2) Prototype,” *2001, 27th International Electric Propulsion Conference*, 2001, pp. 15–19.

[42] Polzin, K., Greve, C., and Sankaran, K., “Pulsed Plasma Acceleration Modeling in Detonation and Deflagration Modes,” *IEPC*, Vol. 893, 2019, pp. 2019.

[43] Eckman, R., Byrne, L., Gatsonis, N. A., and Pencil, E. J., “Triple Langmuir probe measurements in the plume of a pulsed plasma thruster,” *Journal of Propulsion and Power*, Vol. 17, No. 4, 2001, pp. 762–771.